JACS
JOURNAL OF THE AMERICAN CHEMICAL SOCIETY

Article

pubs.acs.org/JACS

Aqueous Self-Assembly of Giant Bottlebrush Block Copolymer Surfactants as Shape-Tunable Building Blocks

Ryan Fenyves,[†] Marc Schmutz,[‡] Ian J. Horner,[†] Frank V. Bright,[†] and Javid Rzayev*[,†]

[†]Department of Chemistry, University at Buffalo, The State University of New York, Buffalo, New York 14260-3000, United States
[‡]Institut Charles Sadron, CNRS-Strasbourg University, Strasbourg 67034, France

Supporting Information

ABSTRACT: Programmed self-assembly of well-defined molecular building blocks enables the fabrication of precisely structured nanomaterials. In this work, we explore a new class of giant polymeric surfactants (M_n = (0.7−4.4) × 10^6 g/mol) with bottlebrush architecture and show that their persistent molecular shape leads to the formation of uniform aggregates in a predictable manner. Amphiphilic bottlebrush block copolymers containing polylactide (PLA) and poly(ethylene oxide) (PEO) side chains were synthesized by a grafting-from method, and their self-assembly in aqueous environment was studied by cryogenic transmission electron microscopy. The produced micelle structures with varying interfacial curvatures and core radii (19−55 nm) boasted rod-like hydrophilic PEO brushes protruding from the hydrophobic PLA cores normal to the interface. Highly uniform spherical micelles with low dispersities were obtained from bottlebrush amphiphiles with packing parameters of ∼0.3, estimated from the polymer structural data. Long cylindrical micelles and other nonspherical aggregates were observed for the first time for compositionally less asymmetric bottlebrush surfactants. Critical micelle concentration values of 1 nM, measured for PEO-rich bottlebrush amphiphiles, indicated an enhanced thermodynamic stability of the produced micelle aggregates. Shape-dependent assembly of bottlebrush surfactants allows for the rational fabrication of a range of micelle structures in narrow morphological windows.

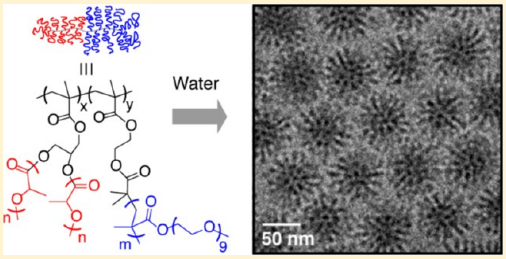

INTRODUCTION

A vast array of functional biological and man-made systems rely on the ability of amphiphilic molecules to self-assemble in aqueous environment, such as cell membranes, drug delivery agents, detergents, oil recovery fluids, and templates for mesoporous ceramics. Just like small molecule surfactants, polymeric molecules containing segments with distinctly different solubility characteristics (lyophilic and lyophobic) can organize into disordered and ordered phases in the presence of a discriminating solvent.[1−3] Polymeric systems possess a number of advantages compared to small molecule surfactants. By virtue of their size, polymeric amphiphiles provide better control over lyophilic/lyophobic balance while generating more thermodynamically stable structures, characterized by lower critical micelle concentrations (CMC) compared to their small molecule analogues.[3] The physical and chemical diversity inherent to organic polymers also allows for the precise tailoring of the generated materials properties. Some commercially available polymeric surfactants, such as block copolymers of poly(ethylene oxide) and poly(propylene oxide), have already found a widespread use as wetting agents, emulsifiers, foam stabilizers, and detergents. The manipulation of interfacial curvature plays a central role in organized soft matter and allows for the fabrication of nanostructures and aggregates with predictable morphologies and physical characteristics. Shape-persistent macromolecules, such as bottlebrush copolymers, provide unique opportunities to control molecular packing and symmetry. This manuscript describes the synthesis and aqueous self-assembly of a new class of giant nonionic surfactants based on bottlebrush copolymers, whose highly tunable two-dimensional architecture (Figure 1) provides unprecedented control over molecular shape, size, and topology.

For small molecule surfactants, Israelachvili et al. analyzed geometrical constraints on self-assembly by using a molecular packing parameter p, defined as $p = v_0/l_0a_{cr}$, where v_0 and l_0 are the volume and the length of the hydrophobic tail, respectively, and a_{cr} is the interfacial area per molecule.[4] Geometrical shapes of micellar aggregates can be predicted by using p, where

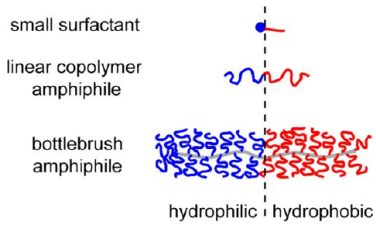

Figure 1. Schematic illustration of bottlebrush amphiphiles, studied in this work, relative to conventional polymeric and small molecule surfactants.

Received: April 1, 2014
Published: May 12, 2014

   dx.doi.org/10.1021/ja503283r | J. Am. Chem. Soc. 2014, 136, 7762−7770

spheres are expected for $p < 1/3$, cylinders for $1/3 < p < 1/2$, bilayers for $1/2 < p < 1$, and inverted structures for $p > 1$. Gruner et al. described the formation of water−lipid mesophases in terms of the competition between the monolayer spontaneous curvature, C_0, and hydrocarbon packing.[5] Similarly, the assembly of amphiphilic block copolymers is governed by the delicate balance between interfacial and conformational contributions to free energy. Pioneering works by Eisenberg et al.[6,7] and Bates et al.[8−11] have significantly contributed to the current understanding of the aqueous self-assembly of linear amphiphilic block copolymers with ionic and nonionic blocks. For a given polymeric system, the interfacial curvature and the aggregate morphology can be tuned by block length asymmetry (Figure 2). Spherical (S) and

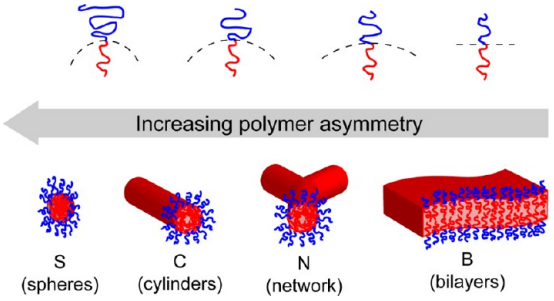

Figure 2. Morphological transitions of linear amphiphilic block copolymers as a function of compositional asymmetry.

cylindrical (C)[12] micelles, Y-junctions, and the network phase (N)[9] and bilayers/vesicles (B)[13] are examples of aggregate morphologies observed for amphiphilic block copolymers in dilute solutions.[2,10,14]

Bottlebrush copolymers are comb-like macromolecules with densely grafted polymeric side chains.[15,16] Excluded volume interactions between side chains lead to extended backbone conformations[17,18] and reduced density of entanglements.[19−21] The cross-sectional diameter and persistence length of cylindrical bottlebrush macromolecules can be manipulated by the length of their side chains.[17,18] Recent developments in controlled polymer synthesis have provided a variety of necessary tools for the preparation of multicomponent bottlebrush macromolecules with exact structural and functional control.[22−28] Owing to their unique comb-like architecture, amphiphilicity can be imparted to bottlebrush copolymers in a number of different ways: radially (core−shell), Janus-like, and blocky, and there has been increasing interest in exploitation of such macromolecular architectures for the preparation of soft materials.[29−33] Notably, Wooley et al. developed the synthesis of poly(acrylic acid)-containing bottlebrush amphiphiles with core−shell and blocky architectures, and investigated their self-assembly in aqueous solutions.[29,34] In a few isolated studies, block copolymer bottlebrush amphiphiles have been shown to produce spherical aggregates often characterized in the dried state,[34−36] which provides insufficient information about the native micelle composition and morphology.

In this manuscript, we demonstrate shape-dependent aqueous assembly of nonionic bottlebrush block copolymer surfactants containing hydrophilic poly(ethylene oxide) (PEO) and hydrophobic polylactide (PLA) branches. Modular variation in the bottlebrush asymmetry, afforded by the utilized synthetic method, allowed us to probe molecular shape−morphology relationships and led to the preparation of highly uniform spherical as well as long cylindrical micelles, which were visualized in the pristine form by cryogenic transmission electron microscopy (cryo-TEM). We believe that these findings will open new avenues in the rational design and fabrication of highly tunable nanostructures. PLA−PEO bottlebrush block copolymers possess an additional advantage of being well suited for biomedical applications due to biodegradability of PLA and biocompatibility of PEO, as demonstrated in their linear copolymer analogues.[37,38]

RESULTS AND DISCUSSION

Polymer Synthesis. Giant bottlebrush surfactants were prepared by grafting from a linear diblock copolymer backbone with latent initiating sites (Figure 3). Hydrophobic PLA

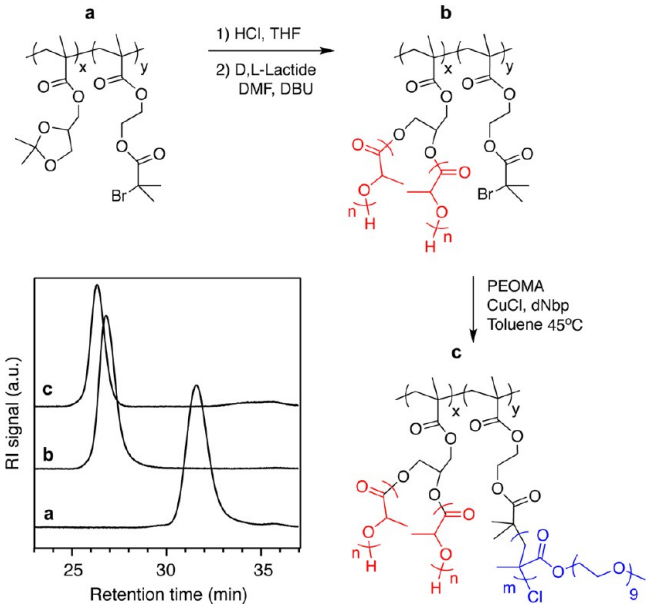

Figure 3. Synthesis and SEC analysis of (a) poly(SM_{95}-*b*-$BIEM_{95}$), (b) poly((SM_{95}-*g*-LA_{24})-*b*-$BIEM_{95}$), and (c) poly((SM_{95}-*g*-LA_{24})-*b*-($BIEM_{95}$-*g*-$PEOMA_{14}$).

branches were installed by DBU-catalyzed ring-opening polymerization of D,L-lactide, while hydrophilic PEO branches were grafted by atom-transfer radical polymerization (ATRP) of PEO_9-methacrylate (PEOMA) from the backbone. This method of installing PEO-like branches using controlled radical polymerization affords modular control over their length with minimal length limitations, unlike methods utilizing linear PEO macromonomers.

Sequential reversible addition−fragmentation chain-transfer polymerization of solketal methacrylate (SM) and 2-bromoisobutyryl methacrylate (BIEM) provided nearly symmetric diblock copolymer backbones poly(SM-*b*-BIEM).[39] Unlike in our previous bottlebrush block copolymer syntheses,[39,40] PLA branches were installed first, anticipating practical difficulties in removing traces of water from highly hygroscopic PEO brushes. Thus, poly(SM) backbone segment was deprotected in acidic THF, and PLA side chains were installed under mild conditions by DBU-catalyzed polymerization of D,L-lactide from the exposed diol functionalities at room temperature.[41,42] Deprotection was confirmed by ^{1}H NMR analysis by the disappearance of solketal signals at 1.30−1.35 ppm and the appearance of hydroxyl signals at 4.75 and 4.95 ppm (Figure

dx.doi.org/10.1021/ja503283r | J. Am. Chem. Soc. 2014, 136, 7762−7770

S1, Supporting Information). The absolute molecular weights of the PLA-grafted block copolymers and the average lengths of PLA branches were measured by size exclusion chromatography (SEC) with a light scattering detector using the dn/dc value of PLA (the analyzed copolymers were composed of >95 wt % PLA). The comparison of the poly(BIEM) signal at 1.98 ppm to the PLA methine peak at 5.18 ppm in the ^{1}H NMR spectra of the copolymers provided the average lengths of PLA branches comparable to those obtained from the light scattering analysis (Figure S2, Supporting Information). Subsequently, ATRP of PEO_9-methacrylate initiated from the α-bromoester groups of the poly(BIEM) segment yielded amphiphilic PLA–PEO bottlebrush block copolymers. From ^{1}H NMR analysis, the average length of poly(PEOMA) branches and the overall bottlebrush composition were calculated by comparing the integrated areas of PEO end group methoxy signal at 3.39 ppm and the PLA backbone methine signal at 5.18 ppm (Figure S2, Supporting Information). Size exclusion chromatography (SEC) analysis corroborated the formation of well-defined copolymers with low dispersities (Figure 3 and Table S1, Supporting Information). The resulting bottlebrush amphiphiles were characterized by molecular weights as high as 4.3 million g/mol. Structural characteristics of the synthesized surfactants are summarized in Table 1.

Table 1. Structural Characteristics of Amphiphilic PLA–PEO Bottlebrushes

polymer	n(PLA)[c]	m(PEOMA)[c]	M_n[d] (kg/mol)	$Đ$[e]
LO-1[a]	24	8	718	1.07
LO-2[a]	24	14	970	1.05
LO-3[a]	24	53	2822	1.05
LO-4[b]	86	8	1654	1.09
LO-5[b]	82	12	1790	1.09
LO-6[b]	82	27	2615	1.09
LO-7[b]	90	56	4350	1.13

[a]Prepared using poly(SM_{95}-b-$BIEM_{95}$) backbone. [b]Prepared using poly(SM_{98}-b-$BIEM_{110}$) backbone. [c]Number of repeat units per branch. [d]Calculated by ^{1}H NMR analysis. [e]Obtained from SEC using polystyrene calibration.

Aqueous Self-Assembly. In this study, the surfactants' composition was controlled by varying the lengths of PLA and PEOMA side chains, while the backbone was kept at a constant length and symmetric. This allowed us to systematically and independently manipulate the cross-sectional diameters of the hydrophobic and hydrophilic ends of the molecule, and to probe the effects of molecular shape on aggregate morphology (Figure 4). Micellization studies were carried out in dilute aqueous solutions (2 wt %) by hydration of the dried copolymer films at 60 °C, which is above the T_g of PLA (48 °C) but below the lower critical solution temperature of PEOMA (90 °C).[43] Amorphous PLA and PEO domains are expected to phase mix in the melt state,[44,45] which was corroborated by differential scanning calorimetry (Figure S3, Supporting Information). Due to the highly hydrophobic nature of PLA ($\chi_{PLA\text{-}water}$ = 3.4),[46] the addition of water to the copolymer films leads to selective hydration of the PEO chains, inducing phase separation. Such a direct copolymer dissolution method has been extensively utilized by Bates et al. for the systematic investigation of nonionic, PEO-containing linear copolymer amphiphiles.[9−11] Low polymer concentrations (<5 wt %) were used to avoid the formation of ordered lyotropic phases,[8] which was not the focus of this work. Aqueous solution aggregates were analyzed by dynamic light scattering to obtain average particle dimensions, and by cryo-TEM to corroborate their exact morphology. Depending on the compositional asymmetry of the bottlebrush surfactants, we observed the formation of spherical micelles with varying sizes and dispersities, cylindrical micelles, and bilayer structures (Table 2). Generally, copolymers with a larger PEO component are expected to form morphologies with progressively more curved interfaces (Figure 4).

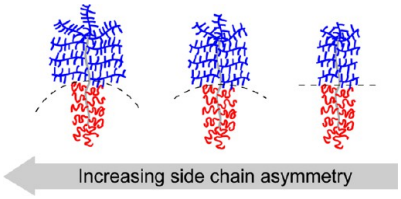

Figure 4. Control of interfacial curvature by bottlebrush side chain asymmetry.

Table 2. Aqueous Self-Assembly Parameters of Amphiphilic PLA–PEO Bottlebrushes

polymer	$w_{sc,PEO}$[a]	morphology[b]	R_{core}[c] (nm)	D_h[d] (nm)	p[e]
LO-1	0.54	S	55 ± 12	250	0.63
LO-2	0.66	S	19 ± 1	100	0.24
LO-3	0.88	S	27 ± 11	190	0.03
LO-4	0.24	B	-	-	1.50
LO-5	0.33	C	30 ± 3	-	0.91
LO-6	0.53	S	40 ± 3	170	0.25
LO-7	0.68	S	20 ± 6	150	0.12

[a]Weight fraction of PEO per side chain. [b]Predominant morphology identified by cryo-TEM (S: spheres, C: cylinders, B: bilayers). [c]The average core radius of spherical micelles (±standard deviation) measured from cryo-TEM images. [d]Volume-averaged hydrodynamic diameters determined by dynamic light scattering. [e]Packing parameter.

Morphology diagrams for linear amphiphilic copolymers are often conveniently depicted as a plot of the weight fraction of one component (representing copolymer's compositional asymmetry) vs the length of the hydrophobic block (related to maximum core dimensions).[10,11] Multidirectional architecture of bottlebrush copolymers presents a challenge in identifying appropriate structural parameters to convey the correct physical meaning in the morphology diagram. We reason that the compositional asymmetry governing the interfacial curvature in bottlebrush copolymers can be described as the weight fraction of PEO per side chain ($M_{sc,PEO}/(M_{sc,PEO} + M_{sc,PLA})$), while the core dimensions can be represented by a total number of repeat units in the PLA backbone and side chains ($N_{b,PLA} + N_{sc,PLA}$). This depiction does not capture the length of the PEO backbone, which seems inconsequential in terms of controlling interfacial curvature due to the highly extended nature of the bottlebrush backbone (vide infra). Plotted using the two parameters described above, the morphology diagram of PLA–PEO bottlebrush copolymers (Figure 5) allows for the direct comparison to linear amphiphilic systems. Similarly to linear systems, spherical micelles are formed for bottlebrush compositions with $w_{sc,PEO}$ larger than 0.5. Decreasing the length of PEO side chains

dx.doi.org/10.1021/ja503283r | J. Am. Chem. Soc. 2014, 136, 7762−7770

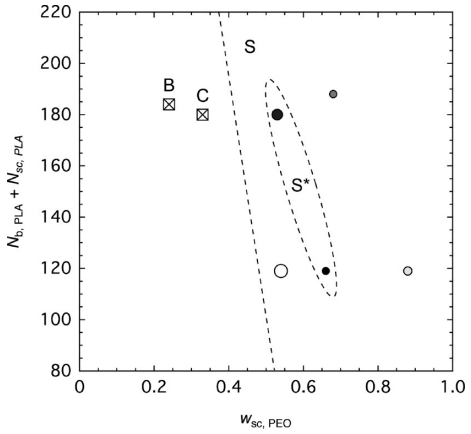

Figure 5. Morphology diagram for PLA–PEO bottlebrush block copolymer amphiphiles in water (B: bilayers, C: cylinders, S: spheres, S*: uniform spheres). The size and shading of circular markers are proportional to the radius and dispersity of spherical micelles, respectively (darker: more uniform).

relative to PLA further leads to morphological transitions to cylindrical micelles and bilayers (polymers 4–7).

Spherical Micelles. Polymers LO-1–3 contained relatively short, identical length PLA side chains and varying length PEO branches. All three polymers formed spherical micelles of different sizes and dispersities when introduced into aqueous medium. Polymer LO-2 produced highly uniform micelles with an average core radius of 19 ± 1 nm, as measured from cryo-TEM images (Figure 6). Hydrophilic, rod-like PEO brushes

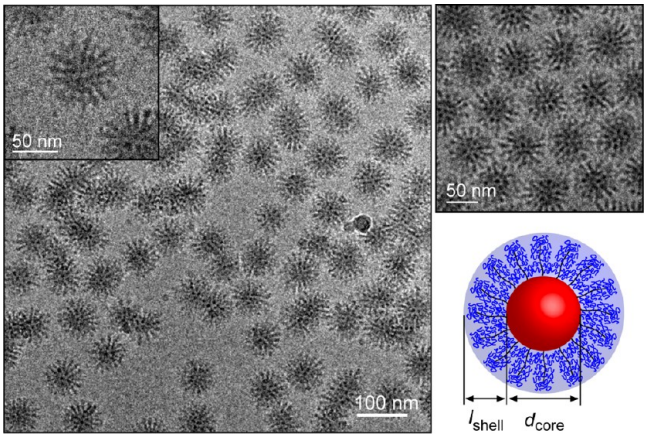

Figure 6. Cryo-TEM analysis of spherical micelles formed from polymer LO-2.

with an average length of ~20 nm are seen protruding from micellar cores normal to the interface. In some sections of the TEM sample with higher micelle concentrations, produced as a result of sample preparation, the micelles appear to organize on a periodic lattice (Figure 6). Both hydrophobic and hydrophilic backbone segments are composed of 95 repeat units each, which translates to a maximum end-to-end distance of 23 nm for a fully stretched polymer chain. The comparison between the maximum attainable length and the measured micellar core radius and corona thickness suggests that bottlebrush backbones carrying both PLA and PEO side chains exist in highly extended conformations. Assuming that density of micelle cores, composed of PLA, is equal to melt density of PLA (1.24 g/mL), the average number of bottlebrush molecules per micelle can be calculated to be 65.

From a volume filling perspective, bottlebrush amphiphiles can be approximated as cones with the cone height equal to the micelle core radius and the cone base area approximated as the cross-sectional area of the hydrophilic brush (Figure 7). Since

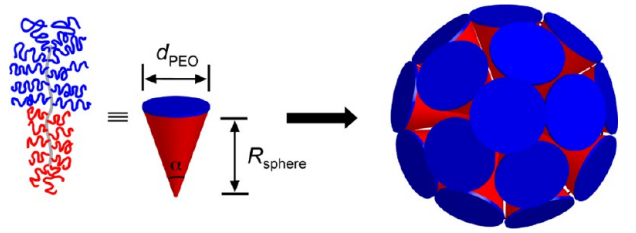

Figure 7. Representation of bottlebrush amphiphiles as cones, and their packing into spherical objects.

side chains in the hydrophilic part of the molecule can be considered bottlebrushes themselves, its cross-sectional radius can be estimated to be 4.4 nm as the length of a fully extended PEOMA side chain plus the hydrodynamic diameter of a single PEOMA monomer extrapolated from the average dimensions of high molecular weight linear PEO in water.[47] Using this analysis, the calculated cone volume of 391 nm^3 is close to the volume of the PLA portion of a single bottlebrush molecule (440 nm^3). Additionally, using the obtained cone angle α = 26.3°, one can calculate the number of cones that are able to pack in a single sphere to be 67, using the following expression:[48]

$$N_{cones} = \mathrm{Int}\left(\frac{2\pi}{3\arccos\left(\frac{\cos\alpha}{2\cos^2\frac{\alpha}{2}}\right) - \pi}\right)$$

A close match between the calculated number of cones per sphere and the aggregation number obtained from cryo-TEM images suggests that polymer 2 provides an ideal composition where the interfacial curvature (and thus particle size) dictated by the side chain asymmetry matches the length of the hydrophobic block. In this scenario, the shape-persistent bottlebrush amphiphiles are able to pack into spherical structures without the need for dramatic conformational changes, which leads to the spontaneous formation of highly uniform micellar aggregates.

Polymer LO-1 boasts shorter PEO branches in comparison to LO-2, and thus is expected to produce aggregates with reduced interfacial curvature, or larger size. As shown in Figure 8a,b, spherical micelles produced from LO-1 are characterized by an average core radius of 55 nm and a large size dispersity (Table 2). The micelle corona is composed of easily discernible rod-like hydrophilic brushes, similar to those produced from LO-2. The core radius is larger than what is physically possible even for a fully stretched backbone and branches (23 + 6 nm), which suggests a composite micelle structure and the presence of (most likely ordered) bottlebrush molecules inside the micelle core that are not part of the interface. The presence of a disk-like morphology, which can account for such a large core radius, is unlikely based on the fact that no nonspherical projections were observed during the cryo-TEM analysis.

dx.doi.org/10.1021/ja503283r | J. Am. Chem. Soc. 2014, 136, 7762–7770

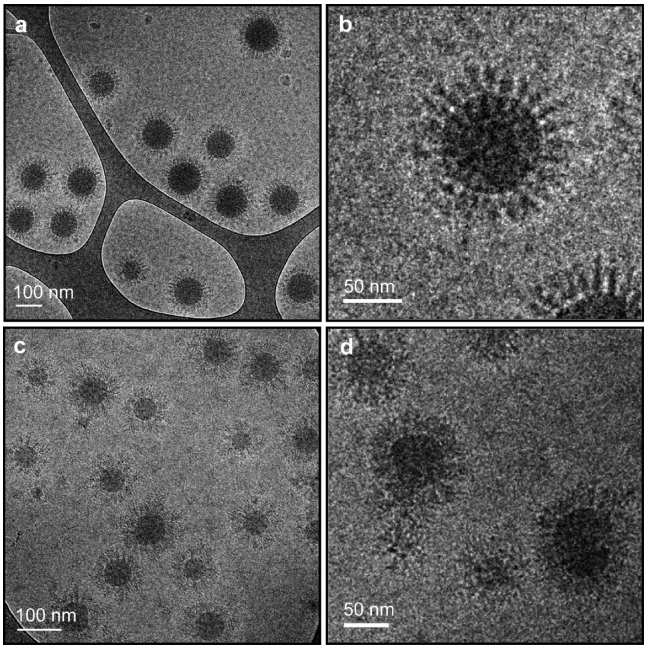

Figure 8. Cryo-TEM images of micelle structures formed from LO-1 (a, b) and LO-3 (c, d).

For linear polymer amphiphiles, chain stretching (and concurrent core dilation) plays an important role in stabilizing a particular morphology for a range of compositions. Once chain stretching cannot compensate for changing polymer asymmetry, a morphological transition occurs.[10] For bottlebrush copolymers, the hydrophobic backbone is nearly fully extended already, and the variation in core dimensions are likely to come from stretching of the side chains at the end of the hydrophobic backbone. For LO-1, PLA side chain in a relaxed conformation has an R_g of 1.4 nm,[49] while a fully stretched side chain can extend as far as 6 nm (end-to-end distance). Thus, the bottlebrush architecture is not very adaptable to changes in the interfacial curvature. We hypothesize that this shape-persistent nature of bottlebrush surfactants leads to narrow morphological windows for simple micellar structures, and to the presence of intermediate regions that produce unusual composite structures, where bottlebrush amphiphiles pack in a shape-dependent manner to minimize free energy.

Polymer LO-3 is more compositionally asymmetric than LO-1, and thus, just based on interfacial curvature arguments, should produce smaller aggregates. However, the micellar cores have to accommodate the extended PLA backbones, and thus physically cannot be much smaller than ca. 19 nm. Such a large mismatch between the spontaneous curvature dictated by the side chain asymmetry and the length of the hydrophobic backbone results in poorly ordered "frustrated" micelles, occasionally adapting nonspherical shapes to accommodate packing frustrations (Figure 8c,d). As a result, the obtained irregular micelles exhibited a large size distribution. The corona of these micelles is thicker (~26 nm) and more diffuse than those derived from LO-1 and LO-2, giving rise to a poorer contrast in TEM, all consistent with much longer PEO side chains.

Polymers LO-4−7 contained longer PLA branches, and thus allowed us to access a much wider surfactant composition window without compromising the bottlebrush architecture. In this series, progressive attenuation of the interfacial curvature by shortening PEOMA side chains resulted in the formation of larger micelles, and subsequently, morphological transitions to cylindrical micelles and bilayers (Table 2). Polymer LO-7, the most asymmetric in the series, formed the smallest spherical micelles with the average radius of 20 nm, close to the minimum possible micelle radius necessary to accommodate hydrophobic PLA bottlebrushes (Figure 9a,b). The diffuse and

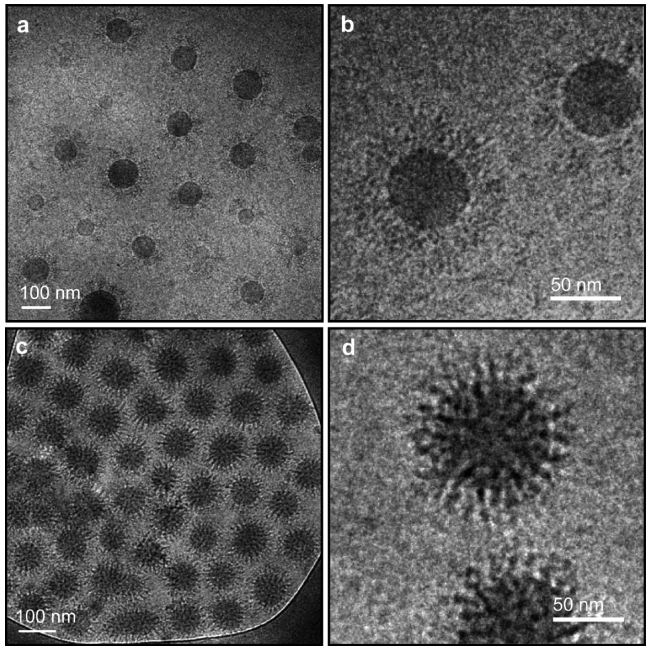

Figure 9. Cryo-TEM images of spherical micelle structures prepared from LO-7 (a, b) and LO-6 (c, d).

thick micelle corona was consistent with long PEO side chains. Using the core radius obtained from TEM images and the volume of the hydrophobic tail, one can calculate the aggregation number for this copolymer to be 20. Even though the average composition ($w_{sc,PEO}$) of this polymer and the micelle core radius was similar to LO-2, the generated micelles exhibited a much broader size distribution. Two factors may contribute to this discrepancy: (1) longer PLA branches in LO-7 render the hydrophobic block with additional conformational freedom, and (2) $w_{sc,PEO}$ may not be the most appropriate term to describe the compositional asymmetry given that PLA branch lengths inside the micelle cores and hydrated PEOMA branches on the outside do not necessarily scale with the number of repeat units in the same fashion (vide infra).

Polymer LO-6, having similar structural characteristics to LO-7 but with shorter PEOMA side chains, exhibited dilated micelle cores with an average radius of 40 nm, consistent with a smaller interfacial curvature produced from a compositionally less asymmetric copolymer (Figure 9c,d). As evidenced by the cryo-TEM analysis, spherical micelles produced from LO-6 were much more uniform, akin to LO-2. The core radius of 40 nm, while larger than the end-to-end distance of a fully stretched PLA backbone (24 nm), could still be attained as a result of PLA side chain stretching (maximum length = 21 nm). The formation of uniform micelles from polymers LO-2 and LO-6 with completely different average compositions ($w_{sc,PEO}$) suggests one or more additional factors more accurately

dx.doi.org/10.1021/ja503283r | J. Am. Chem. Soc. 2014, 136, 7762−7770

describing the spatial asymmetry of the bottlebrush surfactants that in turn govern the interfacial curvature.

Packing Analysis. Similarly to Israelachvili's analysis of small molecule surfactants, we calculated critical packing parameters for bottlebrush amphiphiles using the following equation: $p = V_{PLA}/l_{c,PLA}a_{cs,PEO}$, where V_{PLA} is the volume of the hydrophobic portion of the molecule, $l_{c,PLA}$ is the maximum attainable length of the hydrophobic tail, and $a_{cs,PEO}$ is the cross-sectional area of the hydrophilic part of the bottlebrush (Table 2). The volume of the hydrophobic tail was calculated assuming melt density of PLA (1.24 g/mol), while $l_{c,PLA}$ was obtained by taking into account both the PLA bottlebrush backbone and the side chain lengths $((N_{b,PLA} + N_{sc,PLA}) \times 0.25)$. Due to the brush-on-brush architecture of the hydrated PEO block, it is difficult to estimate its volume and cross-sectional area. Instead, we calculated maximum attainable $a_{cs,PEO}$ by using the length of fully stretched side chains and contribution from the last PEOMA unit at the chain end $(\pi \times (N_{sc,PEO} \times 0.25 + 1.06)^2)$. Given that the side chains in the hydrophilic bottlebrush can be considered bottlebrushes themselves (poly(PEO_9-methacrylate)), this is a good approximation, especially for short side chains. Importantly, it provides us with a quick way to assess packing tendencies of bottlebrush surfactants based on easily accessible structural parameters.

Spherical micelle core radii and their dispersities (represented as coefficients of variation = standard deviation/mean) measured from cryo-TEM images are shown as a function of bottlebrush surfactants packing parameters in Figure 10. No

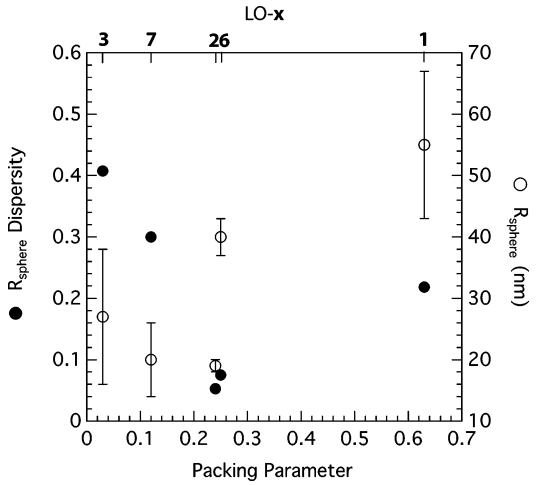

Figure 10. Correlation between the calculated packing parameters and spherical micelle core radii (open circles) and their dispersities (filled circles), obtained from cryo-TEM. Dispersities are represented as coefficients of variation in micelle core radii (std/mean).

matter how asymmetric the polymers are, the observed mean micelle radius does not fall below 19 nm, representing the minimum size necessary to accommodate the PLA backbone. Polymers LO-2 and LO-6, both producing highly uniform micelles, have very similar packing parameters despite having very different average compositions. Clearly, the most uniform micelles (with lowest dispersities) are formed when the packing parameter is close to 0.3, similarly to small molecule surfactants. As a bottlebrush surfactant molecule deviates from this ideal shape, the dispersity of the formed aggregates increases. The results suggest that the shape-persistent nature of bottlebrush amphiphiles is preventing them from adapting to different compositional variations. We believe such a simple analysis on molecular shape can provide guidance in term of designing highly uniform micelle structures with different sizes.

Other Morphologies. As discussed before, the size of spherical micelles obtained from LO-6 is near the maximum that can be accommodated by fully stretching PLA side chains. Decreasing the hydrophilic component of the bottlebrush surfactants by further shortening PEO side chains led to morphological transition, as evidenced by the presence of long cylindrical micelles for LO-5 (Figure 11). Even though both

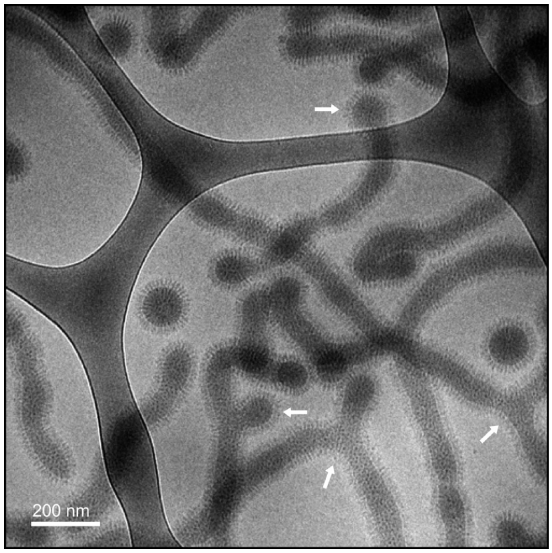

Figure 11. Cryo-TEM analysis of cylindrical micelles prepared from polymer LO-5. Arrows indicate examples of Y-junctions and spherical caps.

LO-5 and LO-6 had nearly identical PLA bottlebrush lengths, the core radius of cylindrical micelles obtained from LO-5 was smaller compared to the spherical micelles obtained from LO-6, indicating chain relaxation as a result of morphological transition. In addition to worm-like micelles spanning more than several micrometers in length, we also observed occasional Y-junctions and spherical caps, typical structural defects associated with cylindrical micelle formation. To our knowledge, this is the first observation of a nonspherical morphology by solution self-assembly of amphiphilic bottlebrush block copolymers, and is highly remarkable due to extremely large molecular weights of the studied copolymers.

The formation of long cylindrical micelles has been attributed to an infrequent birth and rapid micellization mechanism.[50] When micellization kinetics slow down, for example, for higher molecular weight polymers, the formation of structural defects, such as Y-junctions and spherical caps,[51,52] becomes prevalent. It has also been proposed that the packing frustrations associated with deviations from the mean curvature in the Y-junctions are alleviated by chain stretching of high molecular weight polymers.[9] This results in a very narrow morphological window for long cylindrical micelles and the appearance of a network-like morphology, which consists of mostly interconnected Y-junctions, for high molecular weight amphiphilic block copolymers. Remarkably, we observed the formation of high aspect ratio cylindrical micelles from a bottlebrush surfactant whose overall molecular weight $(1.8 \times 10^6$ g/mol) is 2 orders of magnitude higher than those of linear diblock copolymers. We hypothesize that such a behavior can

dx.doi.org/10.1021/ja503283r | J. Am. Chem. Soc. 2014, 136, 7762−7770

be attributed to the inflexible nature of the bottlebrush backbone, which is not able to accommodate packing frustrations in morphologies that have significant deviations from the mean curvature.[53] We speculate that this results in a lower probability of formation of Y-junctions and favors the formation of long cylindrical micelles.

Further decrease in the PEO side chain length (LO-4) resulted in the formation of irregular structures, such as flat bilayers, vesicles, and undulated cylinders (Figure 12). Given

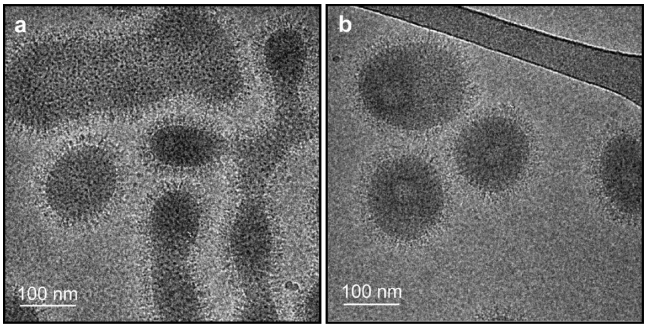

Figure 12. Cryo-TEM analysis of bilayer structures prepared from polymer LO-4.

the rigid nature and large size of bottlebrush amphiphiles, the bending modulus of the obtained bilayers is expected to be high,[54−56] perhaps resulting in very large vesicles not suitable for cryo-TEM analysis. Small vesicles that we were able to observe by cryo-TEM were characterized by a bilayer thickness of ∼40 nm, consistent with the length of two fully extended PLA backbones. The interior of these vesicles is likely composed of highly hydrated PEO chains, enough to provide electron density contrast for TEM analysis.

Micelle Stability. Critical micelle concentration (CMC) is an important parameter characterizing the thermodynamic stability of micellar aggregates. Polymeric micelles often exhibit better stability with CMC values in the μM range compared to small molecule surfactants, which typically show the onset of micelle formation at mM concentrations.[3] More specifically, linear PLA−PEO block copolymers have been reported to exhibit CMC values of 3−7 μM.[57] Producing micelle structures with better stability (lower CMC) allows for their utilization in applications requiring very low polymer concentrations, for example, upon intravenous dilution during drug delivery.[58]

Thermodynamic stability of micellar aggregates formed from bottlebrush surfactant LO-7 was assessed by using the pyrene fluorescence method.[59−61] Briefly, the method relies on the changes in the pyrene excitation and emission spectra based on polarity of the surrounding environment: aqueous below CMC, and hydrophobic above CMC. The pyrene emission I_1/I_3 band ratio decreases as the surrounding medium polarity decreases.[62] It must be noted that LO-7 has the largest PEO content among bottlebrush surfactants producing spherical micelles, while its aggregation number of 20 is among the lowest. For nonionic surfactants, CMC values have been shown to increase with lengthening of the hydrophilic portion of the molecule.[63] Figure 13 illustrates the changes in pyrene emission with polymer concentration. At low surfactant concentrations, the I_1/I_3 band ratio in the emission spectrum levels off at ∼1.75, consistent with pyrene reporting from a largely aqueous environment. The slight deviation of this value from the pyrene signal in pure water (1.9)[64] can be attributed to the

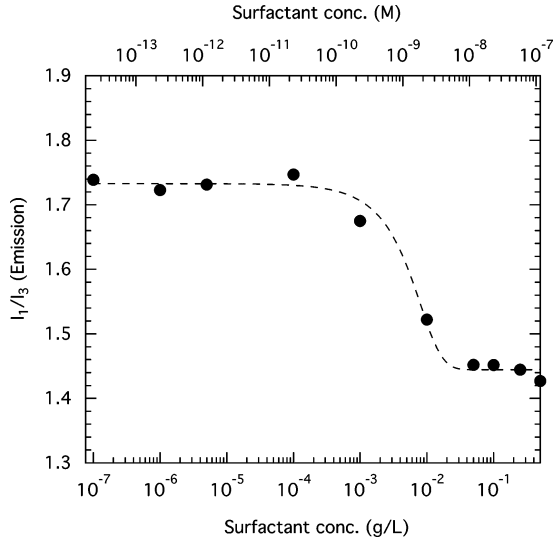

Figure 13. Changes in emission and excitation bands of pyrene co-dissolved with bottlebrush amphiphile LO-7 in water. Pyrene concentration = 5×10^{-7} M.

association of pyrene molecules with the PLA portion of individual bottlebrush unimers. As the polymer concentration increases, the I_1/I_3 band ratio abruptly drops to ∼1.45 due to the entrapment of pyrene molecules inside the micelle cores. This value is slightly higher than the expected band ratio of pyrene in ethyl acetate (1.35),[62] which is similar in structure and polarity to PLA. The results are consistent with previous investigations of polystyrene-PEO micelles, where the discrepancy between the observed pyrene I_1/I_3 band ratio above CMC (∼1.15) and the expected pyrene signal in toluene (1.04)[62] was attributed to the proximity of the core-entrapped pyrene molecules to a polar surface.[64] The transition in the characteristic pyrene emission I_1/I_3 band ratio occurs at a remarkably low surfactant concentration of 1 nM (∼0.005 g/L) with the onset of transition starting at 0.4 nM, which is significantly lower than reported CMC values of linear PLA−PEO copolymers, in terms of both molar and w/v concentrations.[57] The results indicate excellent micelle stability for bottlebrush surfactants, even for those with high PEO content. A detailed investigation of the effect of polymer composition and aggregation number on CMC is currently underway and will be reported elsewhere.

■ CONCLUSIONS

A series of giant nonionic bottlebrush surfactants with varying PLA and PEO side chains were synthesized by a grafting-from approach. When exposed to aqueous environment, bottlebrush amphiphiles assembled into micelle structures, which were characterized by cryo-TEM in their native state. The results revealed shape-dependent aggregation, producing spherical and cylindrical micelles as well as bilayer structures. The micelle core sizes and the length of hydrophilic brushes protruding from the hydrophobic cores were consistent with the presence of highly extended bottlebrush backbones. The average copolymer composition, as captured by components' weight fractions, could not adequately describe the observed self-assembly trends. Packing parameters, calculated from readily available structural data, provided a better correlation between the observed results and the molecular shape. Highly uniform spherical micelles were obtained when the spontaneous

dx.doi.org/10.1021/ja503283r | J. Am. Chem. Soc. 2014, 136, 7762−7770

interfacial curvature, dictated by the side chain length asymmetry in the bottlebrush copolymer, matched the length of the hydrophobic backbone. For the first time, nonspherical morphologies were observed for bottlebrush amphiphiles. Despite their large molecular weights, bottlebrush surfactants generated high aspect ratio cylindrical micelles, which was attributed to their inability to stabilize morphological defects with a significant deviation from the mean curvature.

The observed micelle morphologies and morphological transitions suggest that a typical phase behavior of small molecule surfactants and linear block copolymers can also be expected for bottlebrush amphiphiles. However, the decreased conformational freedom of the shape-persistent bottlebrush surfactants renders them less adaptable to compositional variations and likely results in narrower morphological windows producing highly uniform structures and a richer set of intermediate morphologies. Very low CMC values (~1 nM) measured by the pyrene fluorescence method indicated enhanced stability of micelle structures formed from bottlebrush surfactants. It is important to note that, due to a large size and hydrophobicity of the investigated bottlebrushes, the kinetics of structural evolution toward the global equilibrium are expected to be extremely slow.[11] As such, most of the micellar aggregates likely represent nonequilibrium morphologies. However, the presence of highly uniform spherical micelles with low dispersities and cylindrical micelles with extremely high aspect ratios suggest that a simple phenomenological description based on copolymer structure can be developed and used for rational design of materials, similar to linear block copolymer amphiphiles.

EXPERIMENTAL SECTION

Materials. D,L-Lactide was recrystallized from ethyl acetate, DMF was dried using a commercial solvent purification system (Innovative Inc.), and PEO_9-methacrylate (PEOMA) was passed through alumina column before use. All other chemicals were used without further purification unless stated otherwise. Poly(SM-*b*-BIEM) backbones were synthesized according to the literature procedure.[39]

Solketal Hydrolysis. Poly(SM-*b*-BIEM) (200 mg) was dissolved in 8 mL of THF. Subsequently, 30 drops of 1 M HCl was added to the flask and stirred overnight at room temperature. The mixture was then dried *in vacuo*, dissolved in 2 mL THF and precipitated twice into cold ether to yield 120 mg of white−pink polymer.

Polylactide Grafting. Deprotected Poly(SM_{95}-*b*-$BIEM_{95}$) (100 mg, 0.42 mmol of OH groups), D,L-Lactide (1.03 g, 7.17 mmol) and dry DMF (11.2 mL) were placed in a 20 dram vial equipped with a stirbar and a septum cap. Subsequently, DBU (31 μL, 0.21 mmol) was added to the vial and the mixture was stirred for 1.5 h. The polymerization was quenched with by addition of benzoic acid (10 mg). The mixture was precipitated into water/methanol (50/50 v/v), dried, dissolved in THF, and precipitated in petroleum ether (twice) to produce 652 mg of white powdery polymer.

PEOMA Grafting. CuCl (13.7 mg, 138 μmol), $CuCl_2$ (1.8 mg, 13.4 μmol), 4,4-dinonyl-2,2′-dipyridyl (56 mg, 138 μmol) were mixed, evacuated, and refilled with nitrogen three times. Deoxygenated (bubbled with nitrogen for 30 min) PEOMA/toluene mixture (1:1 v/v, 9.87 mL) was added to the flask containing the catalyst mixture, and the contents were stirred under nitrogen until a homogeneous brown-red catalyst was obtained (2 h). In a separate reaction tube, poly((SM_{95}-*g*-PLA_{24})-*b*-$BIEM_{95}$) (75 mg) was dissolved in a PEOMA/toluene mixture (1:1 v/v, 1.97 mL) and subjected to three freeze−pump−thaw cycles. The catalyst solution (1.97 mL) was transferred to the reaction tube via a nitrogen-flushed syringe under heavy nitrogen flow, and the polymerization was carried out at 45 °C for 18 h. The reaction mixture was then cooled down and precipitated in petroleum ether (4 times), producing 170 mg of bottlebrush copolymer.

Aqueous Self-Assembly. Block copolymers were dissolved in dichloromethane in a 1-dram vial. After the solvent was completely removed under vacuum (1 day), Milli-Q water was added to the vial and the solution was stirred at 60 °C for 2 h.

Cryo-TEM Analysis. Five microliters of the sample was applied onto a 400 Cu grid covered with a lacey carbon film that was freshly glow discharged to render it hydrophilic (Elmo, Cordouan Technologies). The grid was rapidly plunged into liquid ethane slush by using a homemade freezing machine with a controlled temperature chamber. The grids were then mounted onto a Gatan 626 cryoholder and observed under low dose conditions on a Tecnai G2 microscope (FEI) operating at 200 kV. The images were recorded with a slow scan CCD camera (Eagle 2k2k FEI).

Measurements. SEC analysis in DMF (0.1 M LiBr) was carried out at 55 °C on a Viscotek GPC system equipped with a VE-3580 refractive index (RI) detector, two mixed bed (PolyAnalytik) organic columns (PAS-103 M and PAS-105M). The system was calibrated with 10 polystyrene standards from 1.2×10^6 to 500 g/mol. SEC analysis in THF was carried out at 30 °C on a Viscotek GPCMax system equipped with TDA302 teradetector array module containing light scattering, refractive index, ultraviolet, and viscometry detectors and two PolyPore (Agilent) columns. Absolute molecular weights of PLA-grafted copolymers were determined using the light scattering detector and the PLA d*n*/d*c* value of 0.042 mL/g. NMR measurements were preformed on a Varian Inova 500 (500 MHz) spectrometer by using $CDCl_3$ or d_6-DMSO as solvents. Dynamic light scattering (DLS) analysis was conducted on Zetasizer Nano ZS90 (Malvern) at room temperature. Differential scanning calorimetry (DSC) analysis was performed using TA Instruments Q-200 at a heating rate of 10 °C/min.

Steady-state fluorescence excitation and emission spectra were measured with an SLM-AMINCO model 8100 spectrofluorometer. The excitation source was a 450 W xenon arc lamp. Wavelength selectors were double and single grating monochromators, respectively. The spectral band-pass for a given scan was fixed at 1 nm. All spectra were corrected by using appropriate blanks. The blank contribution to the total emission was always <5%.

ASSOCIATED CONTENT

Supporting Information

^{1}H NMR characterization and molecular weight parameters of the synthesized copolymers, DLS histograms of spherical micelles, and DSC characterization of polymer brushes (Table S1, Figures S1−S4). This material is available free of charge via the Internet at http://pubs.acs.org.

AUTHOR INFORMATION

Corresponding Author

*E-mail: jrzayev@buffalo.edu.

Notes

The authors declare no competing financial interest.

ACKNOWLEDGMENTS

This work was supported by the National Science Foundation (DMR-0846584 to J.R., CHE-0848171 to F.V.B.) and by the Kapoor Award (J.R.) from the University at Buffalo.

REFERENCES

(1) Ramanathan, M.; Shrestha, L. K.; Mori, T.; Ji, Q.; Hill, J. P.; Ariga, K. *Phys. Chem. Chem. Phys.* **2013**, *15*, 10580.

(2) Lindman, B.; Alexandridis, P. *Amphiphilic block copolymers: self-assembly and applications*, 1st ed.; Elsevier: Amsterdam, 2000; p 435.

(3) Riess, G. *Prog. Polym. Sci.* **2003**, *28*, 1107.

(4) Israelachvili, J. N.; Mitchell, D. J.; Ninham, B. W. *J. Chem. Soc., Faraday Trans. 2* **1976**, *72*, 1525.

(5) Gruner, S. M. *J. Phys. Chem.* **1989**, *93*, 7562.
(6) Zhang, L. F.; Eisenberg, A. *Science* **1995**, *268*, 1728.
(7) Zhang, L. F.; Eisenberg, A. *J. Am. Chem. Soc.* **1996**, *118*, 3168.
(8) Hajduk, D. A.; Kossuth, M. B.; Hillmyer, M. A.; Bates, F. S. *J. Phys. Chem. B* **1998**, *102*, 4269.
(9) Jain, S.; Bates, F. S. *Science* **2003**, *300*, 460.
(10) Won, Y. Y.; Brannan, A. K.; Davis, H. T.; Bates, F. S. *J. Phys. Chem. B* **2002**, *106*, 3354.
(11) Jain, S.; Bates, F. S. *Macromolecules* **2004**, *37*, 1511.
(12) Won, Y. Y.; Davis, H. T.; Bates, F. S. *Science* **1999**, *283*, 960.
(13) Discher, B. M.; Won, Y. Y.; Ege, D. S.; Lee, J. C. M.; Bates, F. S.; Discher, D. E.; Hammer, D. A. *Science* **1999**, *284*, 1143.
(14) Blanazs, A.; Armes, S. P.; Ryan, A. J. *Macromol. Rapid Commun.* **2009**, *30*, 267.
(15) Sheiko, S. S.; Sumerlin, B. S.; Matyjaszewski, K. *Prog. Polym. Sci.* **2008**, *33*, 759.
(16) Zhang, M. F.; Muller, A. H. E. *J. Polym. Sci.: Polym. Chem.* **2005**, *43*, 3461.
(17) Rathgeber, S.; Pakula, T.; Wilk, A.; Matyjaszewski, K.; Beers, K. L. *J. Chem. Phys.* **2005**, *122*, 124904.
(18) Zhang, B.; Grohn, F.; Pedersen, J. S.; Fischer, K.; Schmidt, M. *Macromolecules* **2006**, *39*, 8440.
(19) Hu, M.; Xia, Y.; McKenna, G. B.; Kornfield, J. A.; Grubbs, R. H. *Macromolecules* **2011**, *44*, 6935.
(20) Tsukahara, Y.; Namba, S.; Iwasa, J.; Nakano, Y.; Kaeriyama, K.; Takahashi, M. *Macromolecules* **2001**, *34*, 2624.
(21) Vlassopoulos, D.; Fytas, G.; Loppinet, B.; Isel, F.; Lutz, P.; Benoit, H. *Macromolecules* **2000**, *33*, 5960.
(22) Beers, K. L.; Gaynor, S. G.; Matyjaszewski, K.; Sheiko, S. S.; Müller, M. *Macromolecules* **1998**, *31*, 9413.
(23) Li, Z.; Zhang, K.; Ma, J.; Cheng, C.; Wooley, K. L. *J. Polym. Sci., Part A: Polym. Chem.* **2009**, *47*, 5557.
(24) Gao, H.; Matyjaszewski, K. *J. Am. Chem. Soc.* **2007**, *129*, 6633.
(25) Runge, M. B.; Bowden, N. B. *J. Am. Chem. Soc.* **2007**, *129*, 10551.
(26) Xia, Y.; Olsen, B. D.; Kornfield, J. A.; Grubbs, R. H. *J. Am. Chem. Soc.* **2009**, *131*, 18525.
(27) Bolton, J.; Rzayev, J. *ACS Macro Lett.* **2012**, *1*, 15.
(28) Huang, K.; Canterbury, D. P.; Rzayev, J. *Macromolecules* **2010**, *43*, 6632.
(29) Li, Z.; Ma, J.; Lee, N. S.; Wooley, K. L. *J. Am. Chem. Soc.* **2011**, *133*, 1228.
(30) Schappacher, M.; Deffieux, A. *Science* **2008**, *319*, 1512.
(31) Hadasha, W.; Mothunya, M.; Akeroyd, N.; Klumperman, B. *Aust. J. Chem.* **2011**, *64*, 1100.
(32) Huang, K.; Jacobs, A.; Rzayev, J. *Biomacromolecules* **2011**, *12*, 2327.
(33) Huang, K.; Rzayev, J. *J. Am. Chem. Soc.* **2011**, *133*, 16726.
(34) Li, Z.; Ma, J.; Cheng, C.; Zhang, K.; Wooley, K. L. *Macromolecules* **2010**, *43*, 1182.
(35) Wu, D.; Zhao, C.; Tian, J.; Zhao, H. *Polym. Int.* **2009**, *58*, 1335.
(36) Yang, Y. Q.; Guo, X. D.; Lin, W. J.; Zhang, L. J.; Zhang, C. Y.; Qian, Y. *Soft Matter* **2012**, *8*, 454.
(37) Saffer, E. M.; Tew, G. N.; Bhatia, S. R. *Curr. Med. Chem.* **2011**, *18*, 5676.
(38) Bhatia, S. R.; Tew, G. N. PLA-PEO-PLA Hydrogels: Chemical Structure, Self-Assembly and Mechanical Properties. In *Degradable Polymers and Materials: Principles and Practice*; Khemani, K., Scholz, C., Eds.; American Chemical Society: Washington, DC, 2012; Vol. *1114*, p 313.
(39) Rzayev, J. *Macromolecules* **2009**, *42*, 2135.
(40) Bolton, J.; Bailey, T. S.; Rzayev, J. *Nano Lett.* **2011**, *11*, 998.
(41) Lohmeijer, B. G. G.; Pratt, R. C.; Leibfarth, F.; Logan, J. W.; Long, D. A.; Dove, A. P.; Nederberg, F.; Choi, J.; Wade, C.; Waymouth, R. M.; Hedrick, J. L. *Macromolecules* **2006**, *39*, 8574.
(42) Mespouille, L.; Nederberg, F.; Hedrick, J. L.; Dubois, P. *Macromolecules* **2009**, *42*, 6319.
(43) Lutz, J. F.; Hoth, A. *Macromolecules* **2006**, *39*, 893.
(44) Nijenhuis, A. J.; Colstee, E.; Grijpma, D. W.; Pennings, A. J. *Polymer* **1996**, *37*, 5849.
(45) Sheth, M.; Kumar, R. A.; Dave, V.; Gross, R. A.; McCarthy, S. P. *J. Appl. Polym. Sci.* **1997**, *66*, 1495.
(46) vandeWitte, P.; Dijkstra, P. J.; vandenBerg, J. W. A.; Feijen, J. *J. Polym. Sci., Part B: Polym. Phys.* **1996**, *34*, 2553.
(47) Devanand, K.; Selser, J. C. *Nature* **1990**, *343*, 739.
(48) Tsonchev, S.; Schatz, G. C.; Ratner, M. A. *Nano Lett.* **2003**, *3*, 623.
(49) Anderson, K. S.; Hillmyer, M. A. *Macromolecules* **2004**, *37*, 1857.
(50) Aniansson, E. A. G.; Wall, S. N.; Almgren, M.; Hoffmann, H.; Kielmann, I.; Ulbricht, W.; Zana, R.; Lang, J.; Tondre, C. *J. Phys. Chem.* **1976**, *80*, 905.
(51) Tlusty, T.; Safran, S. A.. *J. Phys.: Condens. Matter* **2000**, *12*, A253.
(52) Tlusty, T.; Safran, S. A. *Philos. Trans. R. Soc. London, Ser. A* **2001**, *359*, 879.
(53) Matsen, M. W.; Bates, F. S. *Macromolecules* **1996**, *29*, 7641.
(54) Porte, G.; Ligoure, C. *J. Chem. Phys.* **1995**, *102*, 4290.
(55) Bermudez, H.; Brannan, A. K.; Hammer, D. A.; Bates, F. S.; Discher, D. E. *Macromolecules* **2002**, *35*, 8203.
(56) Bermudez, H.; Hammer, D. A.; Discher, D. E. *Langmuir* **2004**, *20*, 540.
(57) Yang, L.; Zhao, Z.; Wei, J.; El Ghzaoui, A.; Li, S. *J. Colloid Interface Sci.* **2007**, *314*, 470.
(58) Owen, S. C.; Chan, D. P. Y.; Shoichet, M. S. *Nano Today* **2012**, *7*, 53.
(59) Zhao, C. L.; Winnik, M. A.; Riess, G.; Croucher, M. D. *Langmuir* **1990**, *6*, 514.
(60) Ray, G. B.; Chakraborty, I.; Moulik, S. P. *J. Colloid Interface Sci.* **2006**, *294*, 248.
(61) Winnik, F. M. *Chem. Rev.* **1993**, *93*, 587.
(62) Karpovich, D. S.; Blanchard, G. J. *J. Phys. Chem.* **1995**, *99*, 3951.
(63) Hsiao, L.; Dunning, H. N.; Lorenz, P. B. *J. Phys. Chem.* **1956**, *60*, 657.
(64) Wilhelm, M.; Zhao, C. L.; Wang, Y. C.; Xu, R. L.; Winnik, M. A.; Mura, J. L.; Riess, G.; Croucher, M. D. *Macromolecules* **1991**, *24*, 1033.